REVERSE TRAJECTORY APPROACH TO COMPUTING IONOSPHERIC CURRENTS TO THE SPECIAL SENSOR ULTRAVIOLET LIMB IMAGER ON DMSP

V.A. Davis, (858) 826-1608, Victoria.A.Davis@saic.com
M.J. Mandell, (858) 826-1622, Myron.M.Mandell@saic.com
Science Applications International Corporation
10260 Campus Point Drive, San Diego, CA 92121

F.J. Rich, (781) 377-3857, Frederick.Rich@hanscom.af.mil
D.L. Cooke, (781) 377-2931, David.Cooke@hanscom.af.mil
Air Force Research Laboratory/VSBX, Space Vehicles Directorate
29 Randolph Road, Hanscom Air Force Base, MA 01731

ABSTRACT

The Special Sensor Ultraviolet Limb Imager (SSULI) was developed by the U.S. Naval Research Laboratory and is deployed on the DMSP F16 polar orbiting spacecraft. The instrument is experiencing a level of noise that is, at times, interfering with its proper operation. The noise is correlated with the spacecraft chassis potential. We computed the potentials about DMSP and the resulting ionospheric currents entering the instrument to determine if the noise could be due to these currents. In order to obtain results of sufficient accuracy, it is necessary to use a reverse trajectory technique that effectively integrates over the thermal distribution of incident ions. The reverse trajectory technique is described in detail. The currents computed using this approach show a strong dependence on the chassis potential that is different from that of the observed noise levels, which suggests that either the noise has another source or other factors reduce the current.

INTRODUCTION

The Special Sensor Ultraviolet Limb Imager (SSULI)[1,2,3,4] was developed by the U.S. Naval Research Laboratory and is deployed on DMSP F16. DMSP F16 was launched into a 830 km sun-synchronous polar orbit on October 18, 2003. The SSULI ultraviolet spectrograph assembly is shown in Figure 1 and Figure 2. Ultraviolet photons enter the instrument, are reflected by the mirror, and then pass through the collimator. They are then reflected by the diffraction grating and enter the microchannel plate detector. The windowless detector is count-rate limited and a loss of gain is expected over time. The collimator is biased +13.5 V with respect to the spacecraft chassis to repel ions.

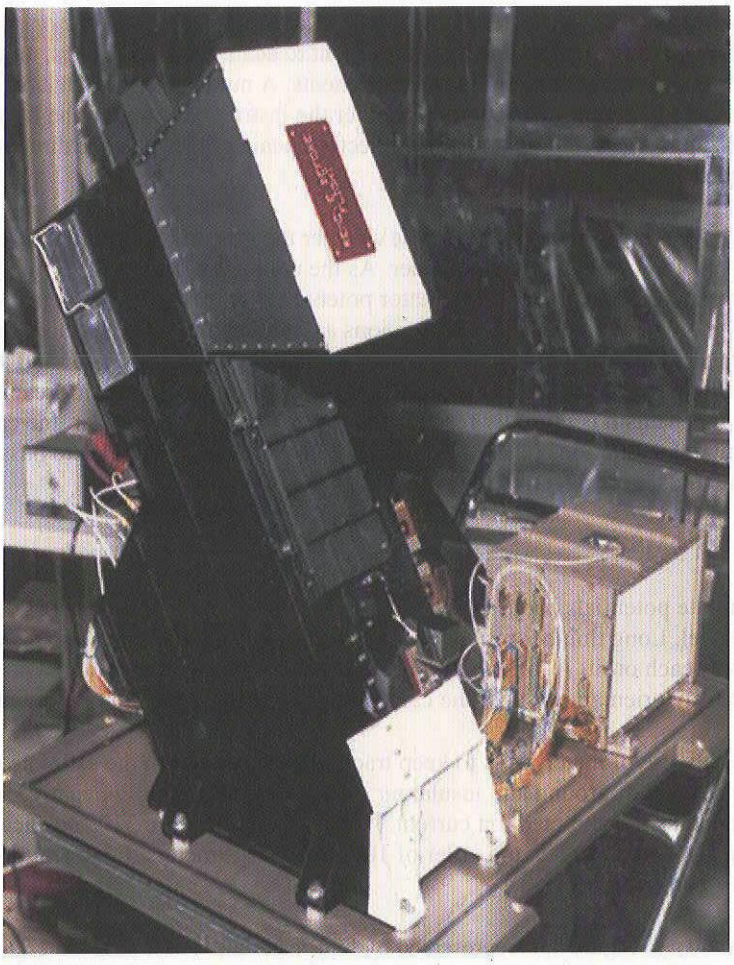

Figure 1. SSULI ultra-violet spectrograph assembly. The white cover over the sunshade opening is removed before flight.

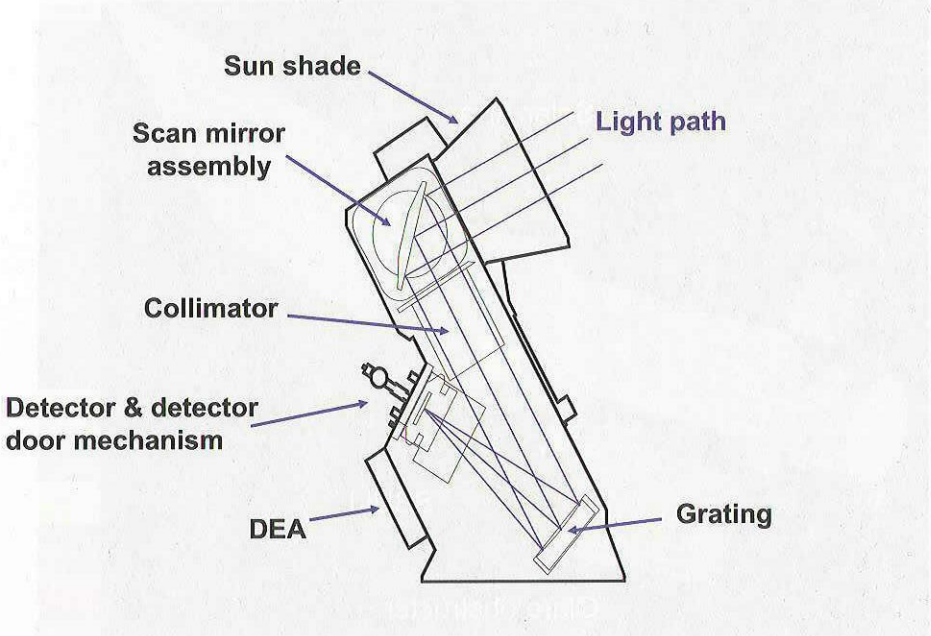

Figure 2. Illustration of the SSULI ultra-violet spectrograph assembly components illustrating the light path.

The instrument is experiencing a level of noise that is, at times, interfering with its proper operation. While data processing techniques are being employed to allow the instrument to achieve its objectives, an understanding of the cause of the noise would allow its elimination on future instruments. A number of mechanisms have been proposed. Here we focus on the conjecture that ionospheric ram ions enter the instrument through the light path and impact the detector. This conjecture is supported by the fact that the detector opening faces the ram direction and the noise is correlated with the spacecraft chassis potential.

The conjecture is that ram oxygen ions (mean energy 4.6 eV) enter the instrument through the light path and generate a signal on impact with the detector in the following manner. As the collimator is at +13.5 V with respect to the chassis, for chassis potentials less negative than -6 V, the collimator potential is at least +7.5 V positive, repelling all the ram ions. For chassis potentials more negative than -16 V, ram ions are attracted to other surfaces and do not reach the collimator. At chassis potentials between -6 V and -16 V ions pass through the collimator and are attracted by the high potential on the detector. Others[5] have shown that some 10 eV ions exiting the collimator reach the detector. The calculations show that this mechanism is *not* fully responsible for the noise. In particular, the calculations show that if the surface potentials are such that ram ions reach the collimator at small enough angles to pass through it, the current remains high at chassis potentials more negative than -16 V.

GEOMETRIC MODEL OF DMSP

We used *Nascap-2k* to compute potentials about DMSP F16 and the resulting currents to SSULI. Figure 3 and Figure 4 show the *Object ToolKit* model. Long thin booms are not included in this model. The solar panel rotates about its support boom by 360 degrees each orbit. A different model is needed for each orientation. The results of this calculation do not depend on the solar array orientation, so all the calculations were done for a single orientation.

For these calculations, the only use of materials is to keep track of surfaces and in the estimate of the surface potentials. Conducting surfaces are at spacecraft ground and insulating surfaces are at a slightly negative potential at which the attenuated electron current equals the attracted ion current. In this model there are 3109 surface elements and 2987 nodes. The average surface element size is on the order of 100 square centimeters. Edge lengths vary from slightly under 1 cm to slightly more than 40 cm.

The interior of the SSULI, shown in Figure 4, is represented by four materials. These four materials are; Shade, which represents the interior of the sunshade; Mirror, which represents the scanning mirror; Collimator, which represents the entrance to the collimator; and Inside, which represents the interior walls between the collimator and the sun shade. As the opening of the collimator is a series of small surfaces at a fixed bias potential, it can be treated as a surface of fixed potential.

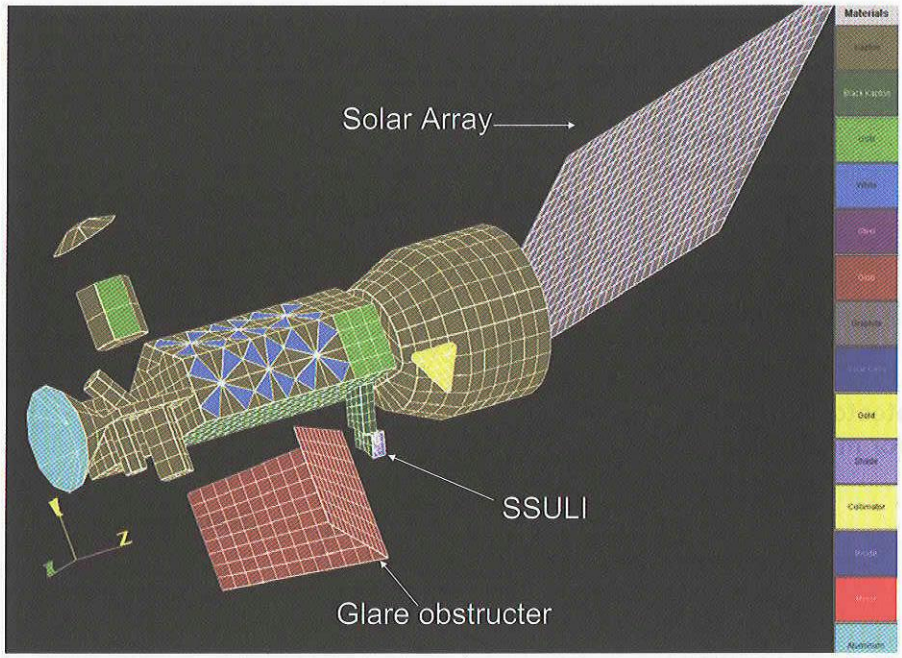

Figure 3. Three-dimensional view of DMSP geometric model.

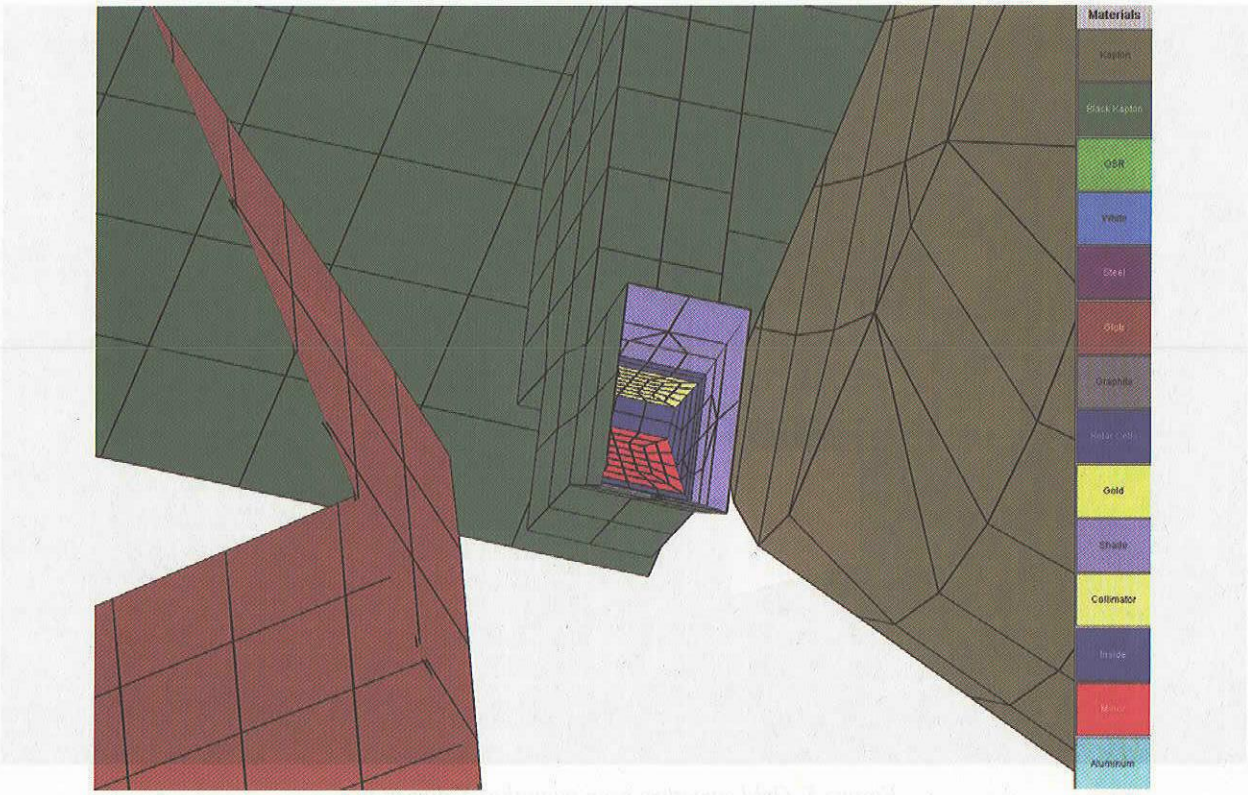

Figure 4. Closeup of three-dimensional view of DMSP geometric model. The red surfaces represent the mirror and the yellow surfaces represent the entrance to the collimator.

ENVIRONMENT

For an 830 km polar orbit, the IRI-90 model gives a range of plasma densities from under 10^{10} m^{-3} to over 10^{11} m^{-3}, with an average near 4 x 10^{10} m^{-3}. The ratio of hydrogen to oxygen varies from 1/40 to 40/1. The electron temperature varies from 0.075 to 0.27 eV, with an average near 0.2 eV.

The spacecraft velocity is 7.4 km/s in the –X direction (in the coordinate system defined by the geometric model). The kinetic energy of an oxygen ion at this velocity is 4.6 eV. The kinetic energy of a hydrogen ion at this velocity is 0.29 eV.

In plasma measurements made by the Special Sensor for Ions and Electrons (SSIES),[6] which is also on DMSP F16, the total plasma density has a wide range of values, with the mid-range value near 2×10^{10} m^{-3}. The O^+ density values are generally, but not always, significantly higher than the H^+ and He^+ values. The spacecraft potentials measured by the SSIES typically range from 0 to -16 V with excursions to more negative values.

In our calculations, we use a density of 2×10^{10} m^{-3} and temperature of 0.2 eV, which gives a Debye length of 0.023 m. The Child-Langmuir sheath thickness for 10 V is 0.55 m. The equilibrium potential of a ram facing insulating surface is -0.46 eV.

A first estimate of the ram current entering the SSULI is the ram current times the projection of the area of the opening in the ram direction. The exposed area, which is reduced from the actual area by both an angle factor and the shadow of the sun shade, is 0.0099 m^2, which gives a ram current of 0.23 μA. The collimator entrance is not directly exposed to the ram, so any ram current that enters the collimator must be reflected by the mirror or other interior surfaces.

GRID STRUCTURE

A spatial grid was constructed about the geometric model. The outer grid has a spacing of 0.5 m, with refinements down to 0.015625 m inside the SSULI. The grid is shown in Figure 5.

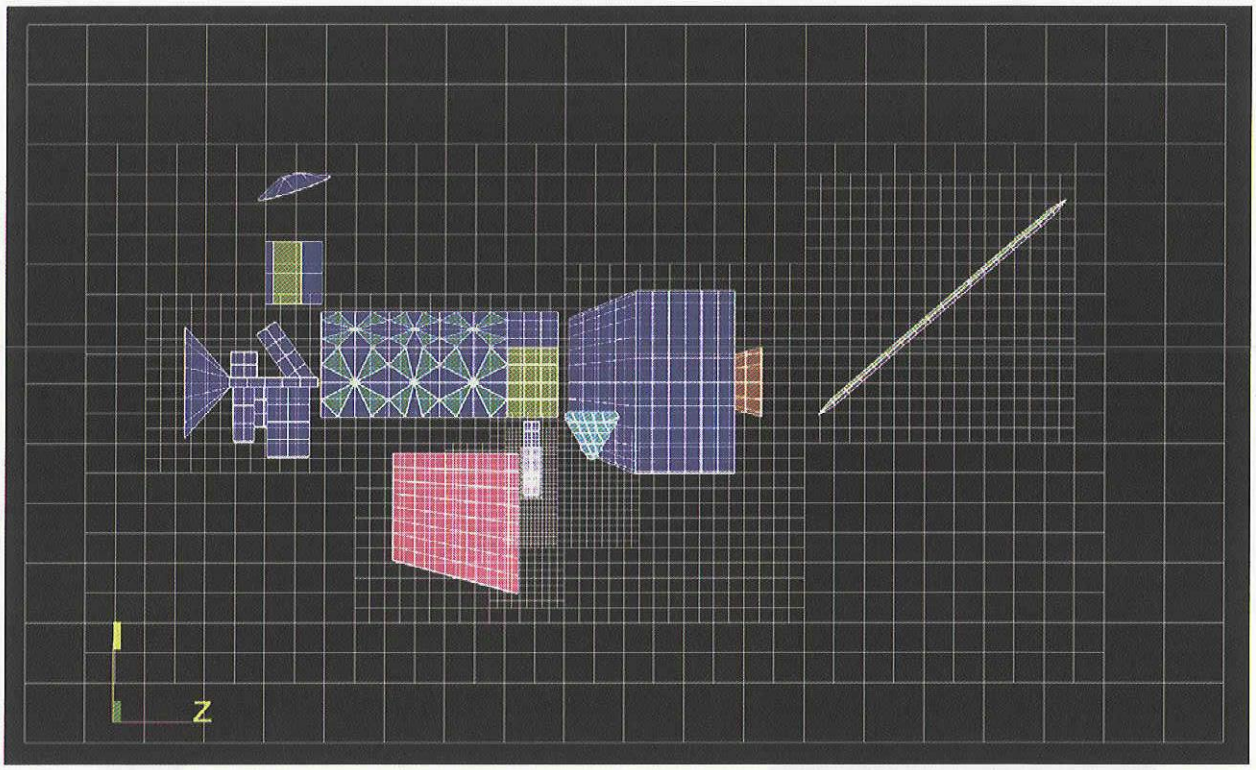

Figure 5. Grid structure seen from the -X direction.

POTENTIALS AND CURRENTS

Surface Potential Boundary Conditions

We used the following potential boundary conditions in our computations of the potentials in the space about DMSP:

- Conductive materials are taken to be at chassis potential.
- The surface potential of insulating materials and ungrounded thermal blankets is slightly negative, generally under one volt, depending on electron temperature, geometry, and orientation with respect to the ram direction. The calculations use a value of -1 V. The outer layer of these blankets is either Black Kapton or Teflon and very few of the blankets are grounded. The ground tabs are tucked in and not attached to chassis ground.[7]
- The exterior of the SSULI is covered with grounded Black Kapton thermal blankets. Black Kapton has a low conductivity that is probably not high enough to conduct away all the incident current of a low-Earth-orbit plasma. Even a grounded Black Kapton blanket is most likely at a slightly negative potential. As our information on the conductivity of Black Kapton is not definitive, one set of calculations was done with the grounded Black Kapton blankets around the SSULI taken to be at chassis potential.
- The opening of the collimator is a screen at +13.5 V with respect to the chassis. This is represented by a surface at +13.5 V with respect to chassis potential.
- The surfaces on the interior of the SSULI and on the interior of the sunshade are anodized aluminum. Moderately thick anodization layers form an insulating surface and therefore are expected to be at a slightly negative potential. If there is a potential barrier that makes it impossible for electrons to reach the surface, the equilibrium potential is +4.6 V, the potential at which the incident ram ion current is repelled. Thin anodization layers do not support differential potentials and are therefore at the potential of the underlying conductor, in this case at the chassis potential. Calculations are done for both assumptions.

- The sun facing surfaces of the solar arrays are set to +20 V with respect to the chassis. This represents an average surface potential. The actual value is not important as these surfaces are too distant from the SSULI to have any direct effect. The current collected by these surfaces is an important factor in setting the chassis floating potential.

Potentials in Space

We computed potentials in the space surrounding DMSP for chassis potentials from -6 V to -22 V and various assumptions regarding the surfaces on the interior and exterior of the SSULI.

Figure 6 through Figure 9 show results for the case with the chassis potential at -14 V, the mirror and other interior surfaces assumed insulating and therefore at -1 V, and the collimator at -0.5 V.

Figure 10 through Figure 12 show results for the case with the chassis potential at -14 V, the interior other than the mirror assumed conducting (and therefore at chassis potential), the mirror at +4.6 V, and the collimator at -0.5 V.

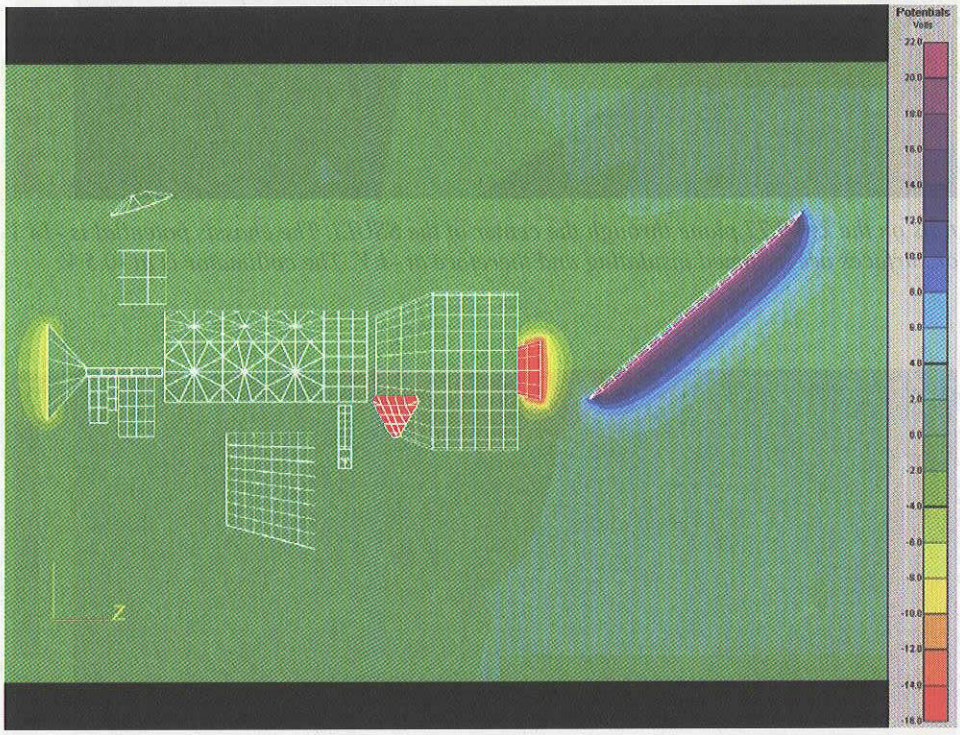

Figure 6. Potentials on the X=0 plane through the center of the object. The chassis potential is -14 V. The mirror and other interior surfaces are assumed insulating and therefore at -1 V. The collimator is at -0.5 V.

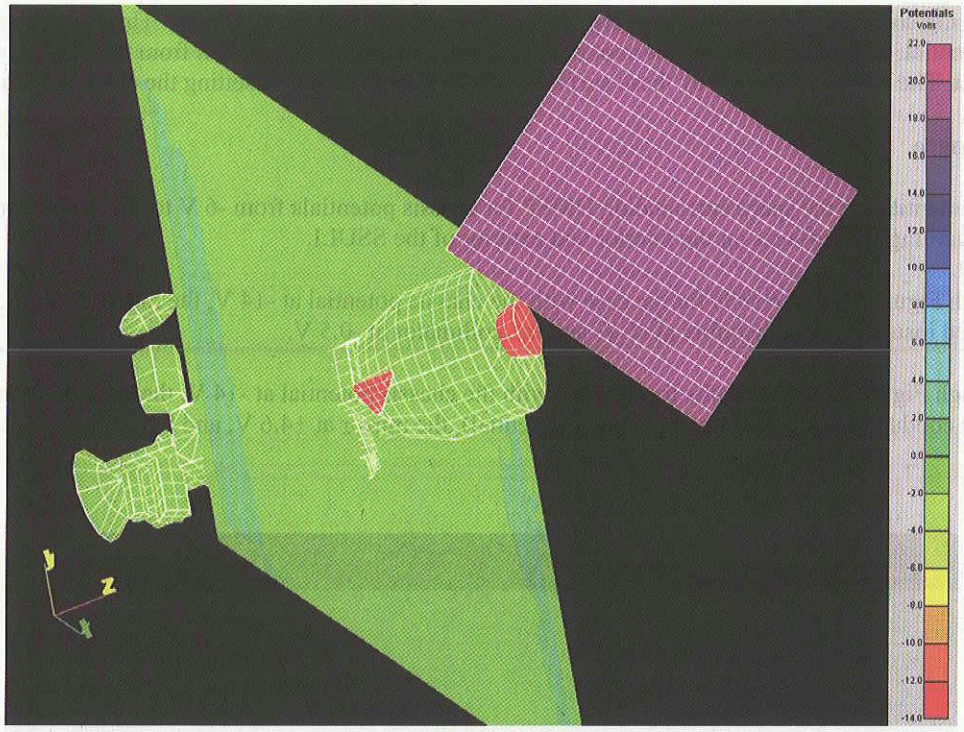

Figure 7. Potentials on the Z=-0.77 plane through the center of the SSULI. The chassis potential is -14 V. The mirror and other interior surfaces are assumed insulating and therefore at -1 V. The collimator is at -0.5 V.

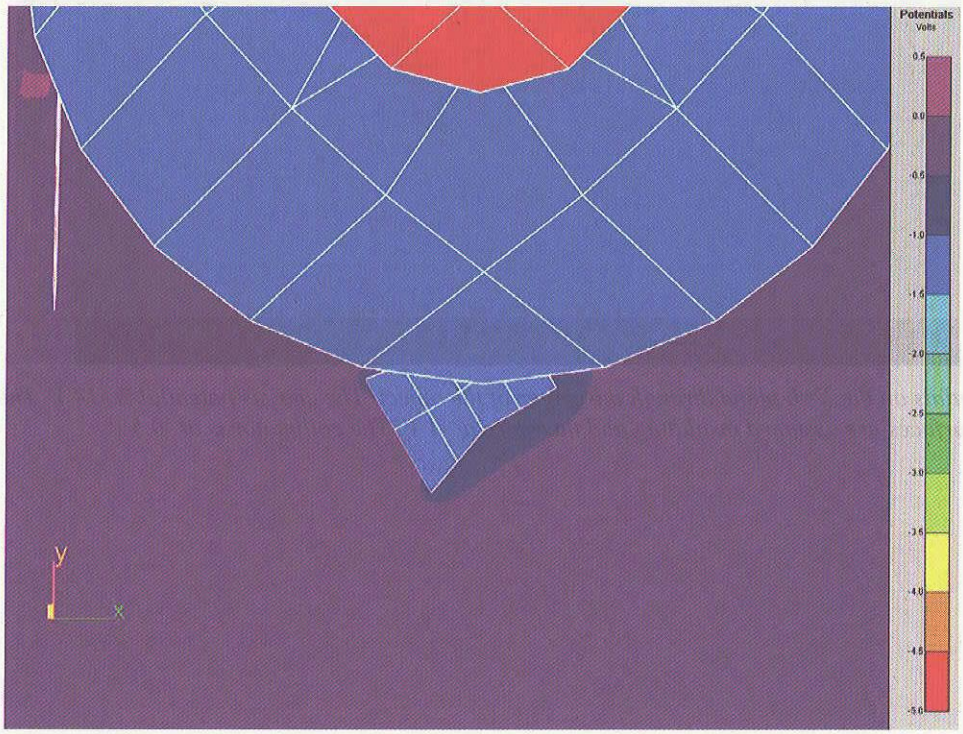

Figure 8. Potentials on the Z=-0.77 plane through the center of the SSULI. Close-up showing SSULI partially obscured by the spacecraft. The chassis potential is -14 V. The mirror and other interior surfaces are assumed insulating and therefore at -1 V. The collimator is at -0.5 V.

Ion Trajectories from Sheath Boundary

Ion currents to surfaces of low-Earth-orbiting spacecraft are often computed by tracking macroparticles from a sheath edge. Figure 9 shows sample ion trajectories from a sheath edge. The view is the same as in Figure 8 above. Oxygen ions enter the instrument and hit the mirror and the interior of the sunshade. In order for these ions to be directly responsible for the noise observed, their trajectories must make a sharp turn and enter the collimator along its axis.

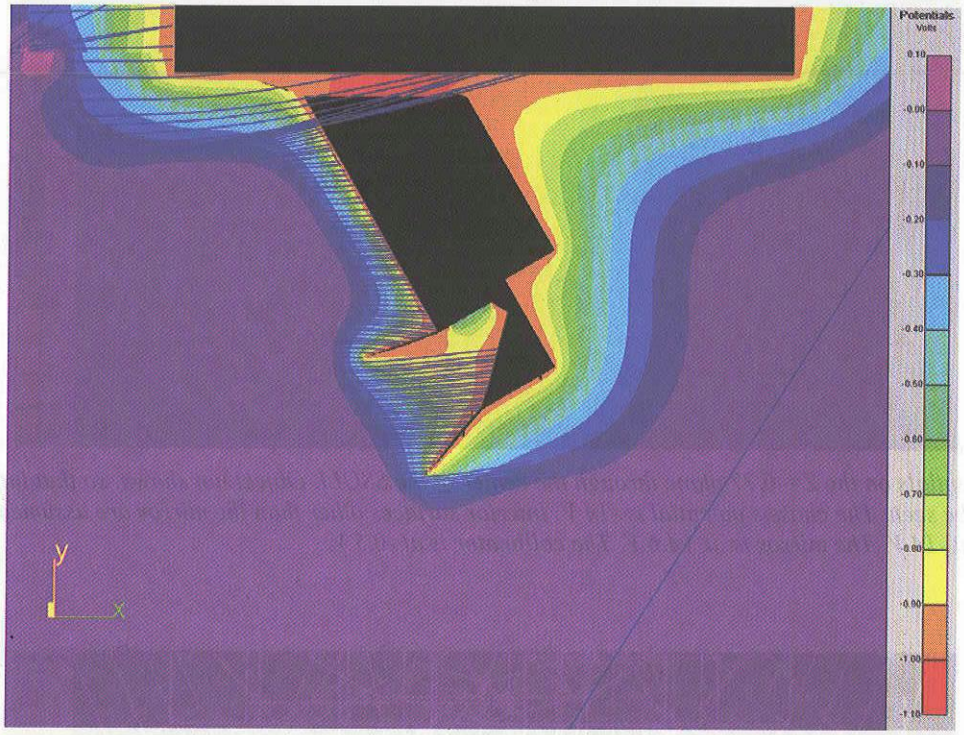

Figure 9. Potentials on the Z=-0.77 plane through the center of the SSULI and trajectories of ram oxygen ions from the intersection of sheath edge and the Z=-0.77 plane. Object not shown so that interior potentials can be seen. The intersection of the object and the plane appear black. Portions of trajectories behind the Z=-0.77 plane are not seen in this view. The chassis potential is -14 V. The mirror and other interior surfaces are assumed insulating and therefore at -1 V. The collimator is at -0.5 V.

A different set of assumptions about the interior materials can give rise to trajectories that enter the collimator along its axis. Figure 10 through Figure 12 show results for the case with the chassis potential at -14 V, the interior other than the mirror assumed conducting (and therefore at chassis potential), the mirror at +4.6 V, and the collimator at -0.5 V. Electrons are excluded by the -11 V potential barrier within the sunshade seen in Figure 10, so isolated surfaces in the interior region rapidly charge to a potential positive enough to repel the incident oxygen ions, +4.6 V. We assume that the surface of the mirror is insulating or poorly coupled to chassis ground, in which case, its surface potential rapidly reaches +4.6 V. In Figure 12, it can be seen that the oxygen ions are reflected by the mirror and impact the side.

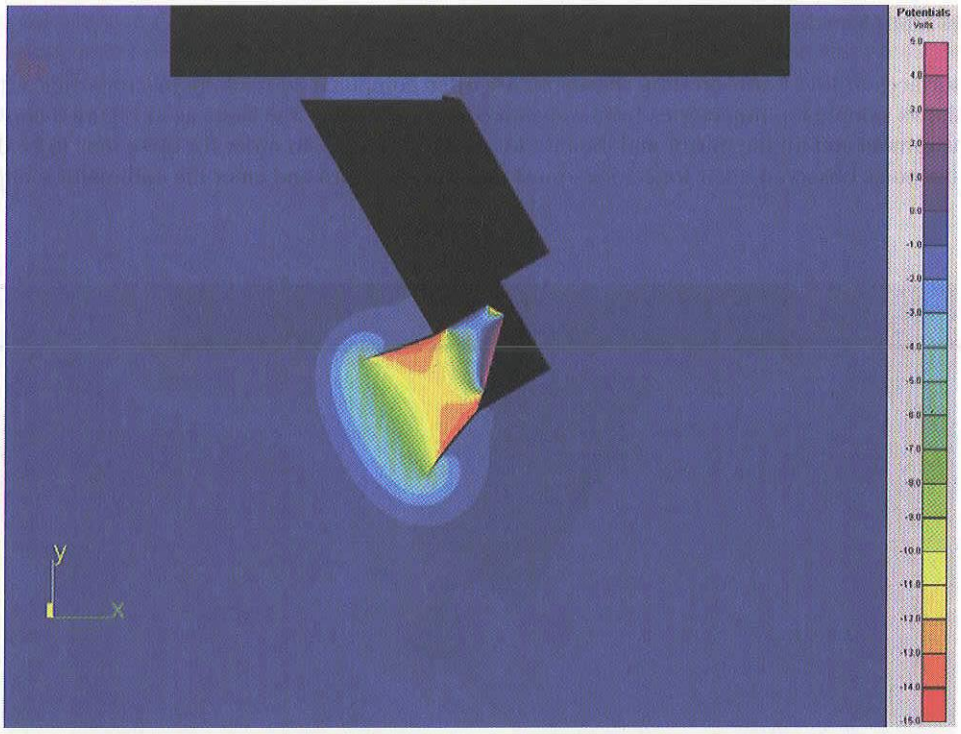

Figure 10. Potentials on the Z=-0.77 plane through the center of the SSULI. Object not shown, so that interior potentials can be seen. The chassis potential is -14 V. Interior surfaces other than the mirror are assumed conducting and therefore at -14 V. The mirror is at +4.6 V. The collimator is at -0.5 V.

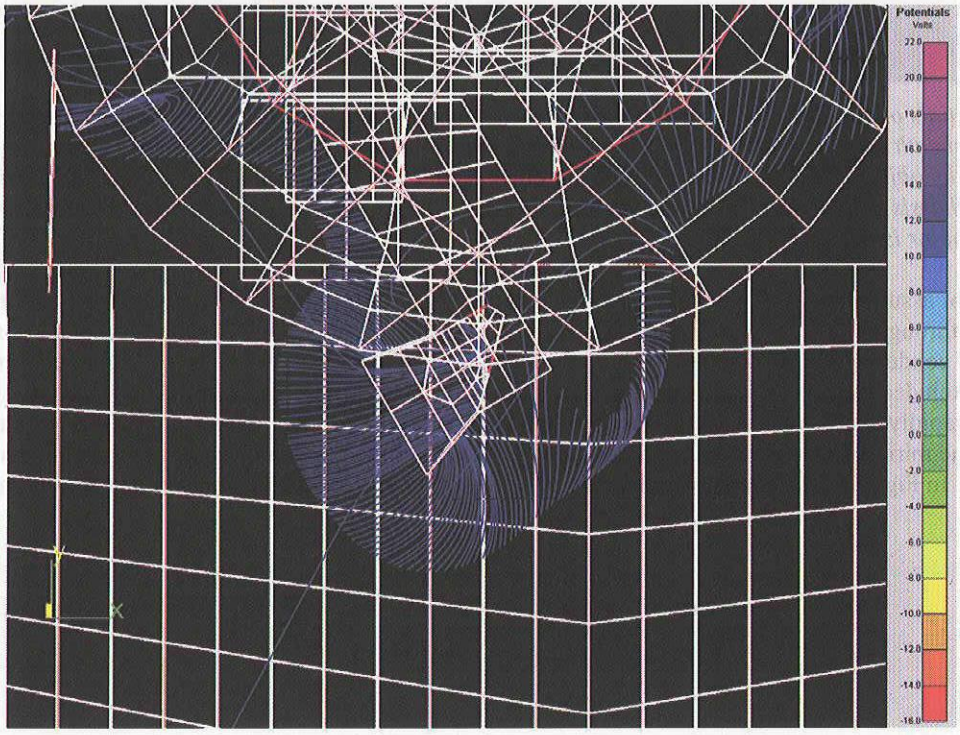

Figure 11. Trajectories of ram oxygen ions from the intersection of sheath edge and the Z=-0.77 plane. Ions are reflected by the mirror. Object shown in outline. The chassis potential is -14 V. Interior surfaces other than the mirror are assumed conducting and therefore at -14 V. The mirror is at +4.6 V. The collimator is at -0.5 V.

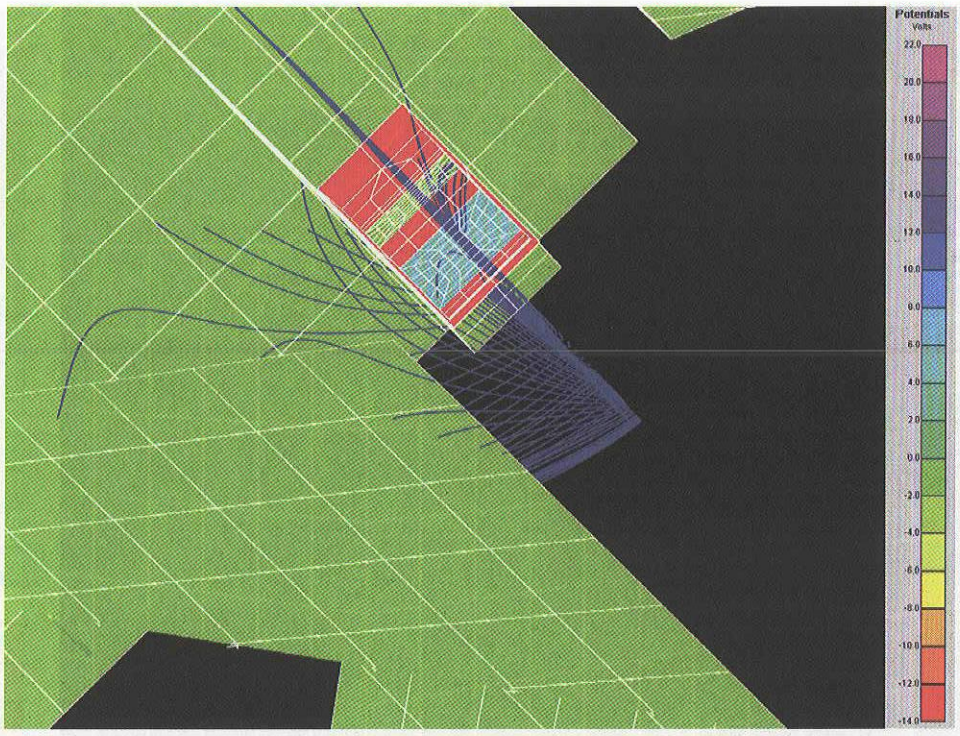

Figure 12. Surface potentials and trajectories of ram oxygen ions from the intersection of sheath edge and the Z=-0.77 plane. Ion are reflected by the mirror and impact the side. The chassis potential is -14 V. Interior surfaces other than the mirror are assumed conducting and therefore at -14 V. The mirror is at +4.6 V. The collimator is at -0.5 V.

Currents

The usual technique used to compute current to spacecraft surfaces in a dense plasma is to track macroparticles from the sheath edge. A limited number of macroparticles with average velocities are assigned current weighting and tracked. This approach works well when the collected current is dominated by particles with velocity near the mean of the distribution function.

However, in this case, the ions normally incident to the collimator opening have original velocities that are far from the mean in both direction and magnitude. This dramatically reduces the accuracy of the calculation. Figure 13 shows trajectories of oxygen ions with 4.3 eV total energy that reached the collimator with velocities within 20° of normal incidence (reverse trajectories). Most of the thirty trajectories originate on the interior surfaces of the SSULI. The six trajectories that do not originate from these surfaces come from a wide range of angles and thus have original velocities far from the mean. In general, trajectories that originate on surfaces are *not* physical particles.

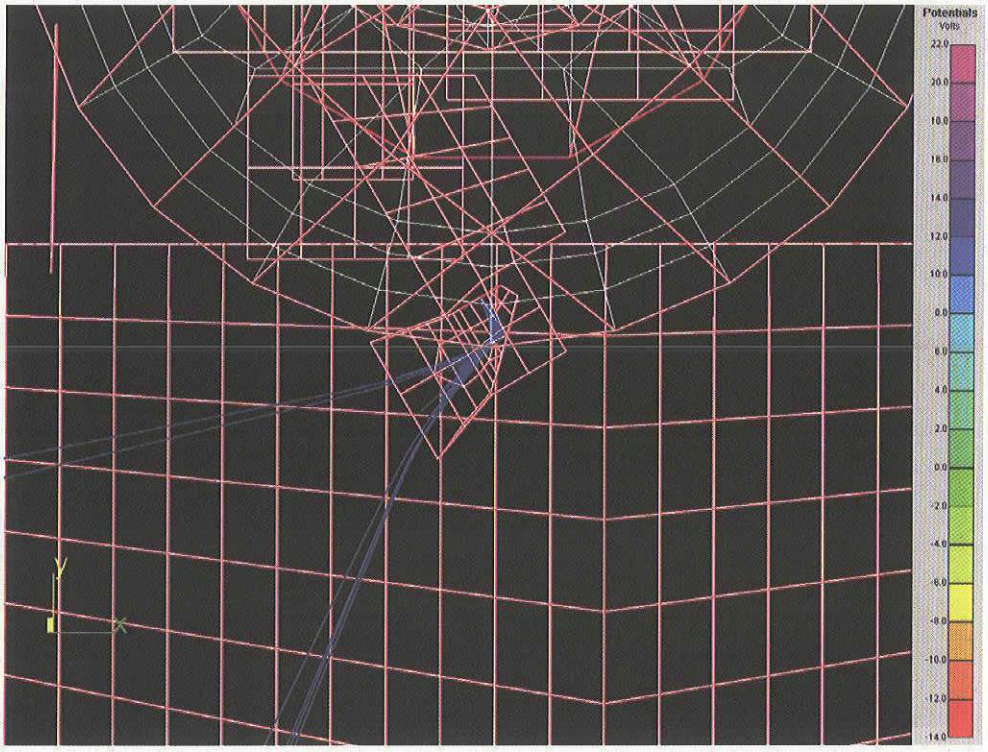

Figure 13. Trajectories of particles within 20° of normally incident on the collimator with a total energy of 4.32 eV. The object is shown in outline. Interior surfaces other than the mirror are assumed conducting and therefore at -14 V. The mirror is at +4.6 V. The collimator is at -0.5 V.

In order to determine the current approximately normally incident to the collimator opening, we need to perform reverse trajectory calculations and integrate over the thermal distribution of the incident ions.

The flux to a specific location at the collimator entrance within 20° ($\pi/9$) of the normal is given by the integral[8]

$$n\left(\frac{m}{2\pi kT}\right)^{3/2}\int_0^{\infty}\int_{\cos(\pi/9)}^{1}\int_0^{2\pi} d\phi\, d\cos\theta\, v^2 dv\,(v\cos\theta)\exp\left(-\frac{m}{2kT}(\mathbf{v}_\infty-\mathbf{v}_o)^2\right),$$

where $\mathbf{v}$, the velocity incident on the collimator entrance, is expressed in spherical coordinates, v, θ, ϕ; $\mathbf{v}_\infty$ is the velocity at infinity; and $\mathbf{v}_o$ is the ram velocity. Portions of phase space for which $\mathbf{v}_\infty$ does not exist do not contribute to the integral. The $\mathbf{v}_\infty$ value corresponding to a $\mathbf{v}$ does not exist whenever the trajectory of the particle with incident velocity $\mathbf{v}$ does not connect with infinity, *i.e.*, intersects the spacecraft. Energy conservation relates the magnitude of $\mathbf{v}_\infty$ to that of $\mathbf{v}$,

$$\frac{m}{2}v_\infty^2=\frac{m}{2}v^2+eV,$$

where V is the potential at the entrance to the collimator. The exponent includes a dot product, which is a function of the angle between the velocity vector at infinity and the ram vector,

$$-\frac{m}{2kT}(\mathbf{v}_\infty-\mathbf{v}_o)^2=-\frac{m}{2kT}\left(v_\infty^2+v_o^2-2\mathbf{v}_\infty\cdot\mathbf{v}_o\right)=-\frac{m}{2kT}\left(v_\infty^2+v_o^2-2v_\infty v_o\cos\psi\right).$$

The cosψ factor is a complicated function of v and in practice can only be determined by tracking macroparticles. The approach we use is to compute the ratio of the flux to the collimator to the flux in the absence of surfaces and potentials.

$$\frac{n\left(\frac{m}{2\pi kT}\right)^{3/2}\int_0^{\infty}\int_{\cos(\pi/9)}^{1}\int_0^{2\pi} d\phi\, d\cos\theta\, v^2 dv\,(v\cos\theta)\exp\left(-\frac{m}{2kT}(v_\infty - v_o)^2\right)}{n\left(\frac{m}{2\pi kT}\right)^{3/2}\int_0^{\infty}\int_0^{1}\int_0^{2\pi} d\phi\, d\cos\theta\, v^2 dv\,(v\cos\theta)\exp\left(-\frac{m}{2kT}(v - v_o)^2\right)}$$

This ratio is computed by generating and tracking a distribution of macroparticles with initial velocities evenly distributed in each of v, cosθ, and ϕ and with weight ($v^3 dv\, d\phi\, \cos\theta\, d\cos\theta$). The ratio rather than the numerator is computed to avoid the necessity for normalization. The quantity

$$\frac{\sum_{v=0}^{v_{max}}\sum_{\cos\theta=\cos(\pi/9)}^{1}\sum_{\phi=0}^{2\pi} v^2\,(v\cos\theta)\exp\left(-\frac{m}{2kT}(v_\infty - v_o)^2\right)}{\sum_{v=0}^{v_{max}}\sum_{\cos\theta=0}^{1}\sum_{\phi=0}^{2\pi} v^2\,(v\cos\theta)\exp\left(-\frac{m}{2kT}(v - v_o)^2\right)}$$

is then computed from the weights and final velocities. The macroparticles included in the numerator are those with θ values less than π/9 that exit the problem space. In the denominator, all the macroparticles are unobstructed and travel in straight lines. The weight and final velocity are printed by the code, so the numerator is easily computed. The denominator is computed when the initial velocities are computed. To get the current into the collimator, this ratio is multiplied by the ram current density, 23.7 μA, times the cosine of the angle of the surface normal with respect to the ram, 0.5 (for 60°), times the surface area, 0.0092 m^2. If the ratio is 0.05, the current into the collimator is 5.5 nA, which is 3.4×10^{10} ions/sec.

A full velocity distribution is generated at each of a distribution of points across the surface in order to determine the ratio for the entire surface.

Figure 14 shows the results of calculations under various assumptions regarding the SSULI surface potentials. The calculations were done with 15 values in each of the two directions along the surface, 30 ϕ values, 18 cosθ values, and 11 speeds from 0 to three times the thermal speed plus the maximum of the ram speed and the speed of a ram ion accelerated by the collimator potential with respect to infinity.

From the figure, we can conclude that at chassis potentials more negative than -14 V, if electrons are excluded, a significant fraction of the ram current enters the collimator and that this fraction increases as the chassis potential drops from -14 V to -22 V with respect to infinity. If all the interior surfaces are insulating, little ram current enters the collimator to the accuracy of the calculation.

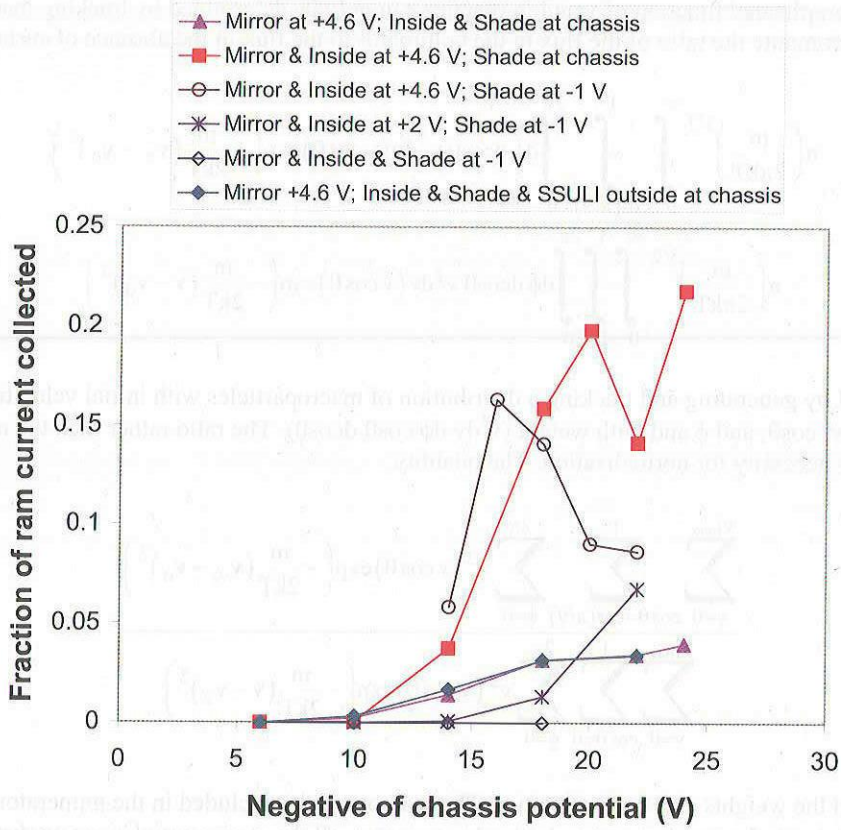

Figure 14. Fraction of ram current collected under various conditions.

CONCLUSIONS

Computing the current to the hidden entrance of the collimator by tracking macroparticles from the sheath edge proved unreasonable as the particles normally incident to the collimator have original velocities that are far from the mean in both direction and magnitude. The reverse trajectory technique efficiently provides definitive current densities to the surfaces hidden from the direct ram flux.

The observed noise in the SSULI instrument, which occurs at chassis potentials from approximately -4 V to -16 V, cannot be fully explained by ram ions that pass through the collimator and along the light path. The chassis potential range over which the noise occurs (-4 V to -16 V) is different than the chassis potential range over which a significant fraction of the ram ions are attracted to and pass through the collimator (-11 V to more negative than -20 V). Our calculations suggest that if some surfaces are effectively conducting enough to create a potential barrier to electrons, more than one percent of the ram current passes through the collimator opening at a small angle for potentials more negative than -11 or -12 V. They also suggest that the fraction remains high at potentials more negative than -20 V.

Figure 14 shows that the ion current entering the collimator at -6 V chassis potential is four to six orders of magnitude less than the ram current. While it is possible that fluxes well under one percent of the ram current are responsible for the observed noise, another phenomenon must be responsible for the cutoff at about -16 V.

REFERENCES

[1] http://www.nrl.navy.mil/tira/Projects/ssuli/.

[2] A C Nicholas, S E Thonnard. Results from the analysis of the refurbished SSULI detector, *Proceedings SPIE*, 3445, p. 527, 1998.

[3] R. P. McCoy, K. F. Dymond, G. G. Fritz, S. E. Thonnard, R. R. Meier, P. A. Regeon, Special Sensor Ultraviolet Limb Imager: An Ionospheric and Neutral Density Profiler for the Defense Meteorological Satellite Program Satellites, *Opt. Eng.*, 33, p. 423,1994.

[4] S. E. Thonnard, S. N. Osterman, R. P. McCoy, J. Z. Williams, K. F. Dymond, N. F. Ferragut, M. A. Doerner, Optical Calibration of the Special Sensor Ultraviolet Limb Imager (SSULI), *Proceedings SPIE*, 2282, p. 98, 1994.

[5] J. Clemmons, private communication.

[6] F. J. Rich and M. Hairston, Large scale convection patterns observed by DMSP, *J. Geophys. Res*, 99, A3, 3827, 1994.

[7] M. Stracko, private communication.

[8] L.W. Parker, Calculation of sheath and wake structure about a pillbox-shaped spacecraft in a flowing plasma, *Proceedings of the spacecraft charging technology conference, 1977*, AFGL-TR-77-0051, NASA TMX-73537, p. 331, 1977.